

A kinetic study of the lipase-catalyzed ethanolysis of two short chain triradylglycerols: alkylglycerols vs. triacylglycerols

Luis Vázquez¹, Oscar Fernandez¹, Rosa M. Blanco², F. Javier Señoráns¹,
Guillermo Reglero¹, and Carlos F. Torres^{1*}

¹Sección Departamental Ciencias de la Alimentación, Facultad de Ciencias,
Universidad Autónoma de Madrid, 28049 Cantoblanco, Madrid, Spain

²Instituto de Catálisis y Petroleoquímica. CSIC. Marie Curie, 2, 28049
Madrid, Spain

*Corresponding author

Telephone: +34 91 4973091

Fax: + 34 91 4978255

E-mail: carlos.torres@uam.es

Abstract

Lipase-catalyzed ethanolysis of two short-chain triacylglycerols, namely tributyrin and 2,3-dibutyroil-1-*O*-alkylglycerols, have been studied. Much faster rate of reaction for the ethanolysis of tributyrin than that of 2,3-dibutyroil-1-*O*-alkylglycerols was attained. A kinetic model for the rate of release of ethyl butyrate and for the inactivation of the lipase has been also studied. The parameter corresponding to the release of ethyl butyrate was one order of magnitude higher for ethanolysis of tributyrin than the corresponding of 2,3-dibutyroil-1-*O*-alkylglycerols.

On the contrary, the stability of Novozym 435 during ethanolysis of 2,3-dibutyroil-1-*O*-alkylglycerols was higher than the corresponding of tributyrin.

At the reaction conditions under study, both ethanolysis reactions take place with high selectivity and yield monoesterified alkylglycerols and sn-2 monobutyryl as the main acylglycerols in the reaction mixtures.

Keywords: *Candida antarctica*, alkylglycerols, ethanolysis, butyric, lipase, kinetics model.

1. Introduction

Alkylglycerols, alkylglycerophospholipids and their derivatives, commonly known as ether lipids, have been the subject of much attention because of their special physiological functions in humans [1, 2]. Ether lipids have been used in the therapy of cancer [3], since they are potent antineoplastic agents which inhibit growth, show antimetastatic activity and induce differentiation and apoptosis in cancer cells [4, 5]. Immune stimulators

properties have also been attributed to dietary ingestion of these substances [6].

In recent years, numerous synthetic ether lipids that do not occur in nature have been prepared to find therapeutic agents such as agonists and antagonists of natural lipid mediators [7]. One example of the mentioned synthetic ether lipids are PAF mimics that retain a short-chain residue esterified at the *sn*-2 position [8].

The studies done during the last decade provide multiple lines of evidence that butyrate indeed interferes with the pathogenesis of colorectal cancer. Butyrate inhibits DNA synthesis and arrests growth of neoplastic colonocytes [9], modifies expression of genes involved in chemotherapy resistance [10] and in cell proliferation/differentiation [11,12], and induces apoptosis [13]. At least some of butyrate's antineoplastic effects in colon cancer cells may be due to its synergistic action with another antiproliferative agent, 1,25-dihydroxyvitamin D3 [dihydroxycholecalciferol; (OH)₂D₃]. In various cancer cell lines it has been shown that butyrate and (OH)₂D₃ act synergistically in reducing proliferation and enhancing differentiation of neoplastic cells [14 , 15].

In spite of its early promise, butyrate is not among the drugs used for cancer treatment. The major problem has been to achieve and maintain its millimolar concentrations in blood. Butyrate is metabolized rapidly as soon as it enters the colonocyte via its active transport system [16, 17, 18], and its plasma concentrations are far below those required to exert its antiproliferative/differentiating actions. Prodrug of natural butyrate, such as tributyrin (TB) and 2,3-dibutyroil-1-*O*-alkylglycerols (SCAKG), are neutral short-chain fatty acid triradylglycerols that are likely to overcome the pharmacokinetic drawbacks of natural butyrate as a drug [19].

In addition, recent studies indicate that butyrate and fish oil work coordinately to protect against colon tumorigenesis [20, 21] Based on these findings, designing new lipidic vehicles structures in which these two fatty acids are incorporated into the body could influence the location of their release and it may allow targeting of these bioactive molecules to specific areas of other tissues.

One of the problems that arise is to elucidate which of these two lipidic vehicles, namely alkylglycerols and triacylglycerols, is more efficient and chemically stable in plasma, diffuses through biological membranes and is metabolized by intracellular lipases, releasing therapeutically effective fatty acids over time directly into the cell.

In a first attempt, the present study focuses on the kinetics of the lipase catalyzed ethanolysis of these two lipidic vehicles containing butyric acid residues. The results obtained fulfill two objectives: 1) show differences in rate of the reaction, selectivity, and provide mechanistic information regarding how these two compounds are recognized by lipases, and 2) lipase-catalyzed ethanolysis of these two triacylglycerol is very useful step for selectively remove fatty acid residues at sn-1, and sn-3 positions and it can be used for subsequent production of structured lipids containing short chain and polyunsaturated fatty acids in a single molecule.

2. Experimental

2.1 Materials

2,3-dibutyroil-1-*O*-octadecylglycerol (SCAKG) was synthesized according to a methodology previously described by our group [22]. Tributyrin (TB) was purchased from Sigma-Aldrich (St. Louis, MO, USA). N-hexadecane for

synthesis was purchased from Merck (Darmstadt, Germany). All solvents used were HPLC grade from Lab-Scan (Dublin, Ireland). The immobilized lipase B from *Candida antarctica* (Novozym 435) was a gift from Novozymes Spain. Mesoporous silica MS3030 was a kind gift from Silica PQ Corporation (PA, USA).

2.2 Ethanolysis reaction.

TB or SCAKG (1,7 g), ethanol (5,3 g) and n-hexadecane as internal standard (0,2 g) were added to a 100 mL flask and mixed by swirling. Then, the lipase 10 % by weight was added. The flask was placed in an orbital shaker at 50 °C and 200 rpm. Samples of 50 µL were withdrawn periodically. The reaction was allowed to proceed for 50 min to 420 min.

2.3 Immobilization of *Candida antarctica* lipase

The protocol of immobilization of lipase has been previously described [23]. Silica MS 3030 was functionalized by reaction with octyltriethoxysilane in toluene, and the octyl-Silica obtained was used as the carrier.

1 mL of ethanol was added for each 100 mg octyl silica and the mixture was left to equilibrate in a closed vial for at least 10 min. 5 mL of the commercial extract of *Candida antarctica* lipase B containing 20 mg protein were dissolved in 25mM phosphate buffer pH 7.0, up to a total volume of 10 mL. After assaying the esterase activity (hydrolysis of p-nitrophenyl acetate followed spectrophotometrically at 348 nm), the enzyme solution was added on the vial containing the silica in ethanol and kept in mild stirring with a helical stirrer. Aliquots from suspension and supernatant were withdrawn at 15 min intervals to assay their respective esterase activities. Final time was determined by the lack of activity, or low constant activity of the

supernatant. The suspensions were then filtered and washed three times with 10mL volumes of 200mM phosphate buffer. The supernatants of the immobilization mixtures, as well as the liquids from these washings, were tested for protein desorption by assays of their catalytic activities (esterasic activity). After the last washing, the derivatives were twice suspended in 10mL dry acetone, filtered out and finally vacuum dried for at least 30 min to ensure a complete drying of the catalyst.

2.4 Analyses of the reaction products by gas chromatography.

The samples were diluted with chloroform to obtain a final concentration lower than 0.1 mg/mL for the subsequent analysis by gas chromatography. Separations were performed on a Hewlett-Packard 5890 series II gas chromatograph with on-column injection using a 7 m 5% phenyl methyl silicone capillary column (Quadrex Corporation, New Haven, CT) (0.25 μm i.d). 12 cm of a 530 μm i.d. deactivated column was used as pre-column. Injector and detector temperature was 43 $^{\circ}\text{C}$ and 360 $^{\circ}\text{C}$ respectively. The temperature program was as follows: starting at 40 $^{\circ}\text{C}$ and then heating to 250 $^{\circ}\text{C}$ at 42 $^{\circ}\text{C min}^{-1}$ with 10 min hold, followed by heating from 250 $^{\circ}\text{C}$ to 325 $^{\circ}\text{C}$ at 7.5 $^{\circ}\text{C min}^{-1}$ with 30 min hold. Helium was used as a carrier gas at a pressure of 5.2 psi. The peaks were computed using GC chemstation software (Agilent Technologies, Santa Clara, CA).

2.5 Mathematical modeling

2.5.1 Reaction rate for the ethanolysis reaction: uniresponse model:

Rate expressions based on a generalized Michaelis – Menten mechanism for the ethanolysis reaction were utilized (Figure 1). A ping-pong mechanism controlled by the rate of deacylation of the enzyme was proposed. These

rate expressions are similar to those described by Malcata et al. [24] and by Lessard and Hill [25] for lipase catalyzed hydrolysis reactions. In particular a modification of these rate expressions, presented by Torres and Hill [26], was employed. The main differences with respect to the model proposed by Malcata et al are: 1) the rate expressions contain the concentration of ethanol rather than the concentration of water; 2) a term for the reverse of the ethanolysis reaction is incorporated in the rate expressions. However, in the present study the reverse of the ethanolysis reaction can be neglected based on the findings that nearly 100 % of fatty acid ethyl esters can be achieved in similar systems [27, 28]. Hence, the rate expression of the model is represented by:

$$\frac{d[G]}{dt} = \frac{v_{\max} [G][B]}{K_m \left(1 + \frac{[G]}{K_m} + \frac{[P]}{K_i} \right)} \quad (1)$$

$[G]$ and $[P]$ are the molar concentrations of the parent acylglycerol, and the lower acylglycerol, respectively. $[B]$ denotes the concentration of ethanol, the v_{\max} is the maximum rate of reaction at a particular glyceride bond $[G]$ at a saturating concentration of the substrate (and in the absence of the other glycerides), the K_m is the Michaelis-Menten constant for the glycerides and the K_i is the inhibition constant for the corresponding ethyl esters. The lumped parameters, v_{\max} , K_i , and K_m are defined as:

$$v_{\max} = \frac{k_2 k_p [E_T]}{k_p + k_{-p}} \quad (2)$$

$$K_i = \frac{k_3}{k_{-3}} \quad (3)$$

$$K_m = \frac{k_{-1} k_{-p}}{k_1 (k_p + k_{-p})} \quad (4)$$

Eq. (1) can be simplified by reparameterization following the approach of Malcata et al. [24] to yield:

$$-\frac{d[G]}{dt} = \frac{\Omega_2[G][B]}{1 + K_1[G]} \quad (5)$$

The corresponding lumped parameters (Ω_2 and K_1) are summarized in Table 1.

2.5.2 Loss of enzyme activity with time

Knowledge of the rate law governing the deactivation process is often important in modeling enzyme-catalyzed processes. For the purpose of modeling, deactivation is usually treated as if it occurs in a single step. It is often assumed that irreversible deactivation of the active enzyme (E) to an inactive form (E_d) obeys first-order kinetics:



The manner in which the enzyme activity varies with time is then given by:

$$a\{t\} = a_0 \exp[-k_d(t - t_0)] \quad (7)$$

where t is time; t_0 is the time at which the first experiment with a particular sample of enzyme is started; $a\{t\}$ is the activity of the enzyme at a particular time t ; a_0 is the activity of the enzyme at time t_0 ; and k_d is the first order deactivation rate constant. The parameter a_0 can arbitrarily be assigned to a value of 1 and subsequent activities are thus normalized with respect to this initial activity.

One of the problems that arise when one tries to evaluate the loss of enzyme activity in batch reactors is the fact that the time of the reaction

and the time at which the set of experiments was started are equivalent. This fact does not permit one to separate the rate of the reaction from the rate at which the enzyme is losing activity. In order to overcome this problem, data sets were obtained using two cycles of reaction with the same batch of lipase in order to distinguish between the times characteristic of the two types of reaction (ethanolysis and deactivation). Each cycle involves the same elapsed time for the ethanolysis reaction but for one step in the cycle, the elapsed time will differ from the time during which the lipase has been susceptible to deactivation ($t - t_0$). The mathematical model used in the analysis of the data thus can account for the effect of deactivation of the enzyme in the combined rate expressions for the rates of ethanolysis reaction.

To characterize the loss of enzyme activity, the variable of importance is the time elapsed since the start of the experiments ($t - t_0$). The amounts of the butyric acid ethyl ester obtained depend not only on the time the reactants in a particular batch are in contact with the lipase, but also the enzymatic activity profile during the time that batch is being processed. Graphical depictions of the resulting functional dependence thus require the use of a three dimensional plot. However, in order to obtain plots that can be more readily interpreted, it is convenient to employ the concept of a pseudo reaction time in order to permit representation of the data in two dimensions [24]. The pseudo reaction time represents a mathematical combination of the time elapsed since the start of the series of experiments and the real reaction time. The pseudo reaction time for a particular batch is defined as

$$t^* = \frac{\int_{t_1}^t a \{ \hat{t} \} d \hat{t}}{a_0} \quad (8)$$

where t^* is the pseudo reaction time, \hat{t} is a dummy variable, t_1 is the time at which processing of the particular batch of interest was initiated, and $(t - t_1)$ is the (elapsed) time during which a particular batch of oil is in contact with the lipase (the actual reaction time). In physical terms when the rate of deactivation of the enzyme is negligible, the pseudo reaction time t^* becomes equal to the actual reaction time $(t - t_1)$. When the rate of deactivation is significant, the difference between the actual reaction time and the pseudo reaction time indicates how much longer the reaction mixture must remain in the reactor to achieve the conversion that would have been achieved if the enzyme had not been partially deactivated. In terms of Equations 7 and 8

$$t^* = \frac{1}{k_d} \{ [\exp \{-k_d(t_1 - t_0)\}] - [\exp \{-k_d(t - t_0)\}] \} \quad (9)$$

Note that as k_d approaches zero, the difference in the exponential terms approaches $k_d(t - t_1)$ and t^* approaches $(t - t_1)$. The reader should also note that the value of $(t_1 - t_0)$ represents the sum of the times that the enzyme was used as a biocatalyst in previous trials and the total time necessary to recover the catalyst in the various filtration steps prior to its use in the trial of interest.

3. Results and discussion

3.1 Direct comparison between lipase-catalyzed ethanolysis of tributyrin and sn-2,3-dibutyroil-1-O-alkylglycerols.

The weight percentage of ethyl butyrate from the reaction mixtures released during the first 40 minutes of both ethanolysis reactions is shown in Figure 2. It can be observed that the rate of lipase-catalyzed ethanolysis of TB is much faster than that of SCAKG. A higher reaction rate can be expected in the case of tributyrin compared to that of SCAKG because of the fact that TB contains three butyric acid residues and SCAKG only two. However, inspection of the course of the reaction indicates that after 15 minutes of reaction, the percentage of ethyl butyrate released is ca. 10% and 50% for ethanolysis of SCAKG and TB respectively. These results indicate that lipase-catalyzed ethanolysis of TB is approximately five times faster than lipase-catalyzed ethanolysis of SCAKG.

3.2 Time course of the ethanolysis of SCAKG and TB in the presence of Novozym 435

The course of the ethanolysis of SCAKG and TB in the presence of Novozym 435 is depicted in Figure 3A and 3B respectively. Two trials reutilizing the same batch of lipase were effected in both cases. The differences observed between the two trials assayed for each ethanolysis reaction could be, in part, attributed to partial inactivation of the lipase and were utilized to determine the inactivation constant according to the methodology described in the *Mathematical modeling* section. Besides the differences in reaction rates between ethanolysis of SCAKG and TB discussed before, it can be observed that monoesterified alkylglycerols reach a plateau after 60 minutes of ethanolysis reaction that it is maintained almost constant during the course of the reaction. This result indicates that at these reaction conditions, Novozym 435 is highly selective for butyric acid residues located at sn-3 position. On the contrary, this plateau is not observed in the case of

ethanolysis of TB. In this case, 1,3-dibutyryn is rapidly transformed in 2-monobutyryn. This observation is consistent with that by Piyatheerawong et al [29].

Inspection of Figures 3A and 3B again indicates the difference in reaction rates among the two ethanolysis reactions studied. Hence, the percentage of SCAKG and TB after 20 minutes of reaction was ca 50 % and below 1 % respectively.

3.3 Kinetics modeling of the lipase-catalyzed ethanolysis of SCAKG and TB

It should be noted that the kinetic model utilized in the present study only includes parameters for the forward reaction and inhibition effects. Hence, to avoid overparametrization, facilitate the non linear regression analysis and based on the findings that nearly 100 % of fatty acid ethyl esters can be achieved in similar ethanolysis reaction systems, Equation 5 does not account for reversibility of the reaction that was considered to be negligible. In this study, in an attempt to improve the results of the ethanolysis reaction towards SCAKG, a second lipase (a lipase from *Candida antarctica* immobilized on mesoporous silica) was also utilized for the ethanolysis of SCAKG. The kinetic parameters obtained are shown in Table 2.

Inspection of the Table 2 indicates that the parameter corresponding to release of butyric ethyl ester (Ω_2) is an order of magnitude smaller for ethanolysis of SCAKG than the corresponding for ethanolysis of TB. A higher value of this parameter was attained with the immobilized *Candida antarctica* on mesoporous silica which indicates that this lipase is slightly faster than Novozym 435 in ethanolysis of SCAKG.

Negative values for K_1 were obtained in the three cases under study. Because the lumped parameter K_1 involves a difference of two terms, namely, $\frac{1}{K_m}$ and $\frac{1}{K_i}$ (Equation 1), negative values can be obtained for K_1 .

Regarding the inactivation of lipases the lowest value of k_d was obtained for ethanolysis of SCAKG catalyzed by Novozym 435. In this case, the contribution to the fitting of k_d was almost negligible and similar results were attained removing this parameter from the model. This result indicates that *Candida antarctica* lipase is very stable at this reaction conditions, and numerous trials reusing the same batch of lipase should be necessary to get enough data to characterize the activity decay and properly calculate the value of k_d for this lipase. For that reason the value reported that corresponds only to two consecutive trials, it is an estimate that should be used for comparison purposes but not to determine the extent of the lipase inactivation. Unfortunately, a higher value of k_d was observed for ethanolysis of SCAKG catalyzed by the immobilized *Candida antarctica* on mesoporous silica.

These results indicate that the immobilization process on *Candida antarctica* lipase has two opposite effects: 1) increases the rate of release of butyric acid ethyl ester (higher value of Ω_2) and 2) has a deleterious effect on the stability of the biocatalyst (lower value of k_d in comparison with that attained with Novozym 435).

In addition, inspection of Table 1 also indicates a relatively high deactivation constant for ethanolysis of TB that can be attributed to an additional

deleterious effect caused by tributyrin that does not take place in ethanolysis of SCAKG.

The estimated half-life of the lipases under study according to the values of k_d attained are 180, 35, and 10 hours for ethanolysis of SCAKG catalyzed by Novozym 435, ethanolysis of SCAKG catalyzed by the immobilized *Candida antarctica* on mesoporous silica, and ethanolysis of TB catalyzed by Novozym 435 respectively.

3.4 Kinetic model of the release of ethyl butyrate

Curves corresponding to fits of kinetics model for release of ethyl butyrate are shown in Figure 4.

The model contains the assumption that deactivation of the enzyme (E) obeys first order kinetics. Hence, the kinetics model corresponds to combination of equation (5) with a first order deactivation term. The reader should also note that the data points correspond to two different trials in which the same enzyme was reused (after recovery from the previous trial). To facilitate inspection of the data, different symbols have been utilized for the data from the two different trials considered in the analysis. The data points corresponding to the same elapsed time within a given trial are characterized by a shift on the pseudo reaction time scale that depends on the extent of inactivation of the lipase. It can be observed that no shift in the pseudo reaction time was observed for the shorter reaction times. The extent of inactivation can only be noticeable at the longer reaction times. Hence, for example for the ethanolysis of SCAKG catalyzed by *Candida antarctica* lipase immobilized in mesoporous silica (Figure 4B), the reaction time 420 minutes is shifted to a pseudo reaction time of 392 and 340 minutes for the first and the second trial respectively. On the contrary, for

the ethanolysis of SCAKG catalyzed by Novozym 435 (Figure 4A) no significant shift in the pseudo reaction time is observed at 30 minutes of reaction time for both trials. On the contrary even higher lipase activity is observed at short reaction times which could indicate that other factors (such as recovery of the lipase and experimental errors) could partially interfere with the reported value of k_d . It should be also indicated that the extent of the inactivation, to be perceptible, should be significantly higher than the experimental error in each trial.

For these reasons (very short reaction times and experimental errors) it is not possible to graphically visualize the extent of inactivation for the ethanolysis of TB catalyzed by Novozym 435.

Inspection of Figure 4A indicates that ethanolysis of SCAKG catalyzed by Novozym 435 occurs in two stages: a first rapid release of ethyl butyrate during the first hour of reaction followed by a second stage with slower release of ethyl butyrate. This effect could be attributed to inhibition effect for accumulation of monoesterified alkylglycerols or ethyl butyrate in the surroundings of the active site of Novozym 435. This phenomenon was not clearly observed neither for ethanolysis of SCAKG catalyzed by *Candida antarctica* lipase immobilized in mesoporous silica (Figure 4B) nor for ethanolysis of TB catalyzed by Novozym 435 (Figure 4C).

4. Conclusions

A very efficient methodology for the ethanolysis of two different triacylglycerols has been attained. Much faster rate of ethanolysis for TB than for SCAKG was observed.

High regio-selectivity of Novozym 435 was observed for the ethanolysis of SCAKG with a rapid accumulation of monoesterified alkylglycerols in the

reaction mixture that is maintained almost constant the remaining time of the reaction.

The kinetic model developed in this study indicates that the parameter corresponding to release of butyric ethyl ester (Ω_2) is one order of magnitude higher for the ethanolysis of TB compared to that for the ethanolysis of SCAKG which confirms the experimental observation of the time course of both reactions.

Finally, low inactivation rate was observed for ethanolysis of SCAKG in the presence of Novozym 435 ($k_d = 3.82E-03$). Based on this parameter, the estimated half-life of the lipase is 180 hours, which permit to reutilize the same batch of lipase up to 20 trials.

In conclusion the kinetic model developed in the present study indicates differences in rate of the reaction, selectivity, and provide mechanistic information regarding how these two triacylglycerols are recognized by lipases. In addition, lipase-catalyzed ethanolysis of these two compounds is very useful step for selectively remove fatty acid residues at sn-1, and sn-3 positions and it can be used for subsequent production of structured lipids containing short chain and polyunsaturated fatty acids in a single molecule.

5. Acknowledgements

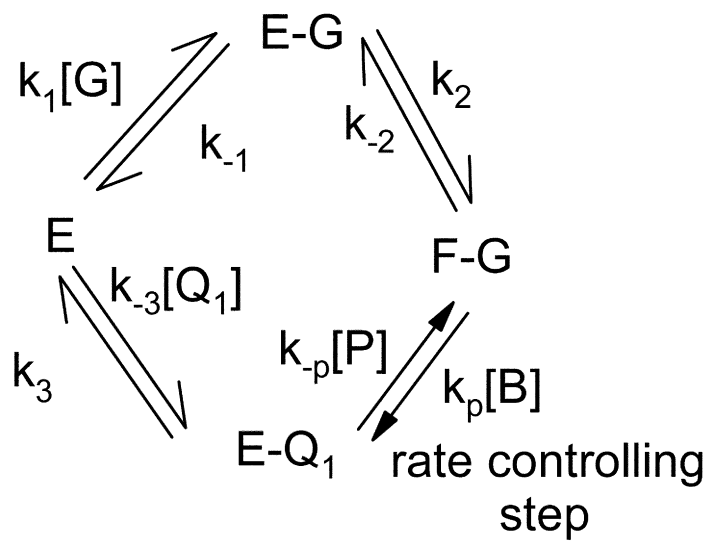
This work was supported by the projects AGL2006-02031/ALI and AGL2008-05655 by Ministerio de Ciencia (Spain) and also by Comunidad Autonoma de Madrid (ALIBIRD, project number S-505/AGR-0153) and Consolider-Ingenio FUN-C-FOOD (CSD2007- 00063). A predoctoral fellowship for Luis Vázquez, provided by Comunidad Autonoma de Madrid, is also acknowledged.

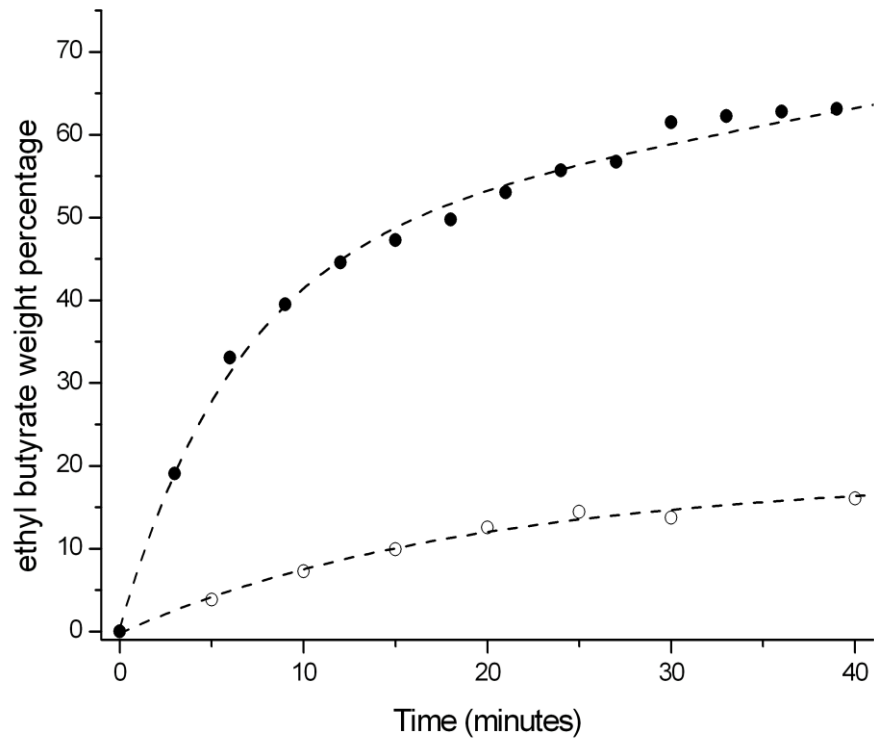
Table 1. Definitions of model parameters in terms of the intrinsic rate constants.

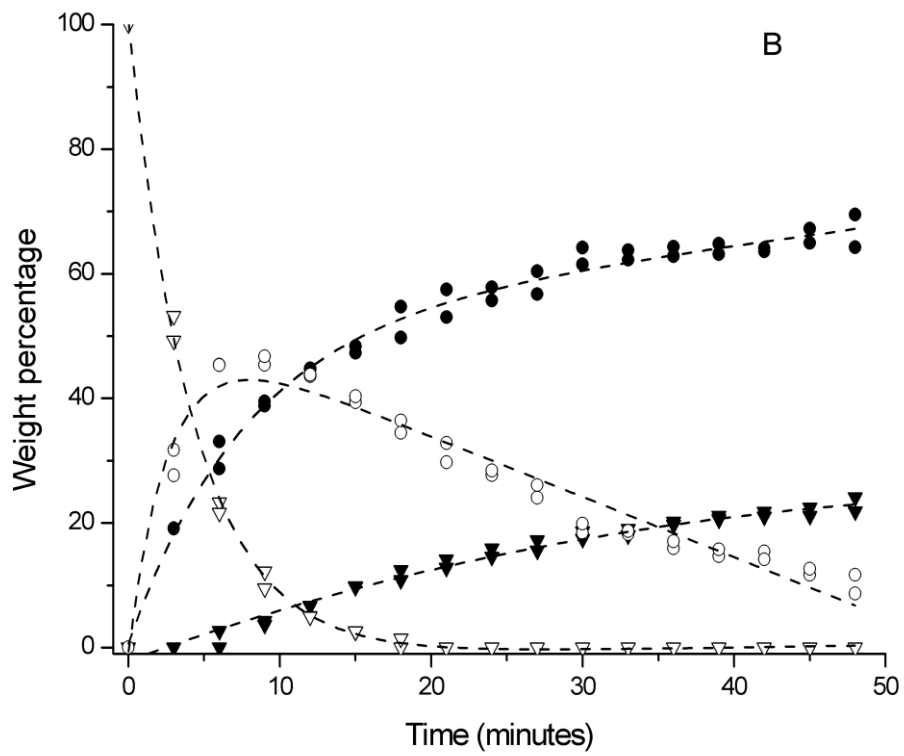
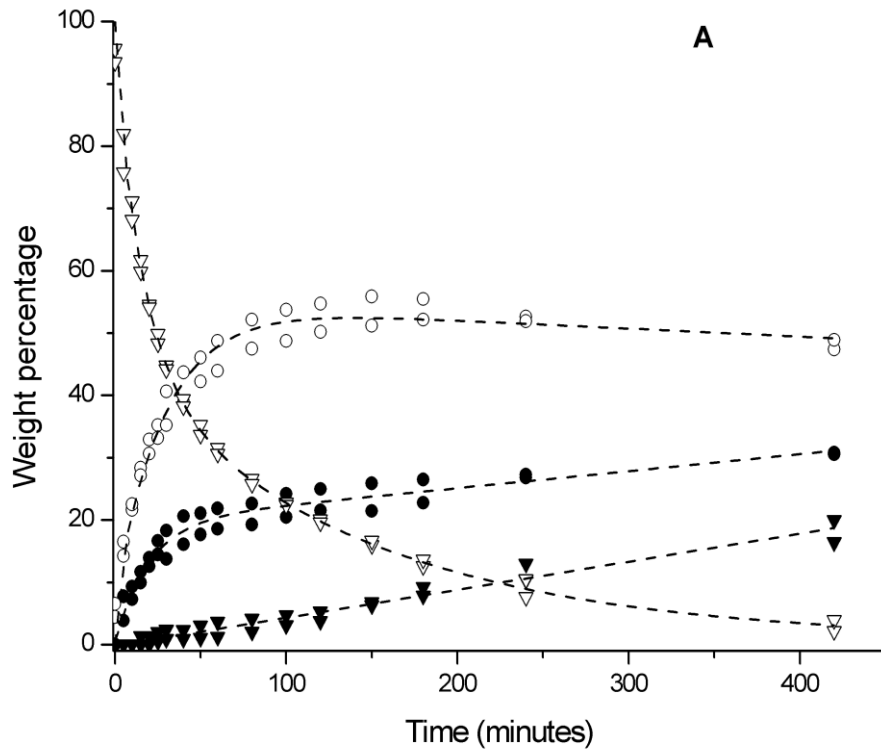
Parameter	mechanistic interpretation
Ω_2	$\frac{k_p k_1 k_2 [E_T]}{k_{-1} k_{-2} \Delta}$
K_1	$\frac{1}{\Delta} \left(\frac{k_1}{k_{-1}} + \frac{k_1 k_2}{k_{-1} k_{-2}} - \frac{k_{-3}}{k_3} \right)$
Δ	$1 + \frac{k_{-3}}{k_3} [G_0]$

Table 2. Parameter estimates for the best fits of lipase-catalyzed ethanolysis of two short chain alkylglycerols and triacylglycerols

Parameter	SCAKG Novozym435	SCAKG Immobilized <i>C. antarctica</i>	TB Novozym435
Ω_2	4.73E-06±1.94E-06	1.17E-05±1.16E-06	3.29E-05±7.22E-06
K_1	-1.38E-03±9.05E-08	-1,34E-03±5,08E-05	-4.93E-04±1.62E-08
k_d	3.82E-03±1.71E-03	2.22E-02±2.66E-03	7.60E-02±8.08E-03







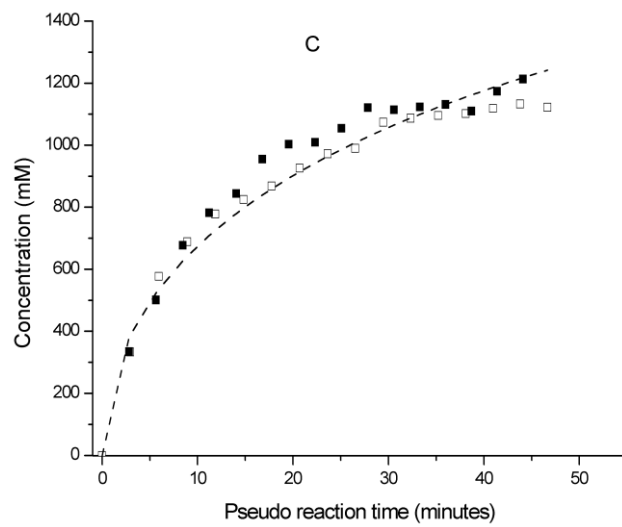
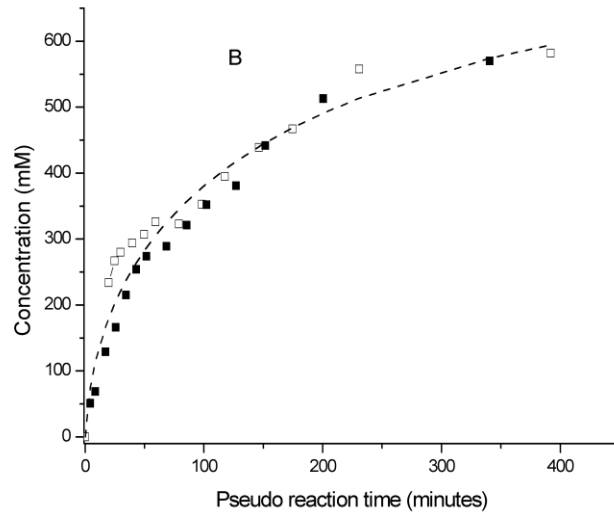
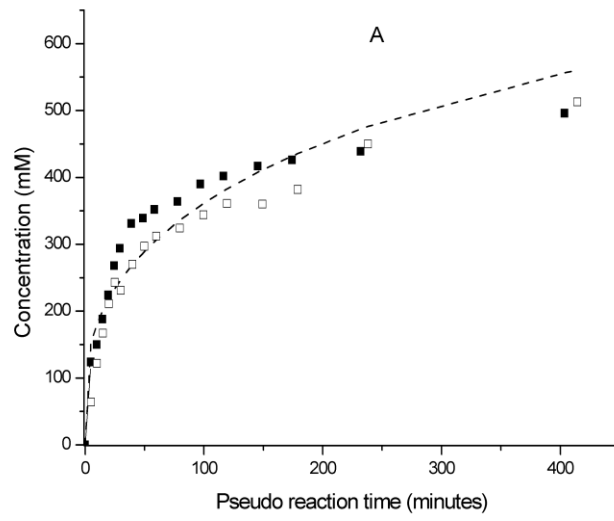


Figure captions

Figure 1. Schematic representation of the ethanolysis reaction. E = enzyme, G = glyceryl ester bond (reactant glyceride), E-G = activated form of the enzyme and the native ester bond, F-G = covalent transformed form of the enzyme and the native ester bond, E-Q = activated form of the enzyme and the fatty acid ethyl ester, B = ethanol, P = lower glyceride liberated from the native ester, Q = fatty acid ethyl ester. k_1 , k_{-1} , k_2 , k_{-2} , k_p , k_{-p} , k_3 , k_{-3} , are rate constants.

Figure 2. Comparison between the rate of release of ethyl butyrate in lipase-catalyzed ethanolysis of tributyrin and short-chain alkyglycerols. filled symbols correspond to tributyrin, Open symbols correspond to short-chain alkyglycerols.

Figure 3. Lipase-catalyzed ethanolysis of short-chain alkyglycerols (A) and tributyrin (B). Figure 3A: open triangles: SCAKG; open circles: mono-esterified alkyglycerols, filled circles: ethyl butyrate, filled triangles: non-esterified alkyglycerols. Figure 3B: open triangles: tributyrin, open circles: dibutyryn, filled circles: ethyl butyrate, filled triangles: monobutyryn.

Figure 4. Curves corresponding to fit of kinetics model for lipase-catalyzed ethanolysis of short-chain alkyglycerols in the presence of Novozym 435 (A), in the presence of *Candida antarctica* immobilized on mesoporous silica (B) and ethanolysis of tributyrin in the presence of Novozym 435 (C). Dashed lines correspond to fitted values. Open symbols correspond to trial 1 and filled symbols correspond to trial 2.

Bibliography

- [1] H. K. Mangold, in Snyder, FL. (eds). Ether Lipids. Chemistry and biology. New York: Academic, 1972, pp. 157-176.
- [2] P. T. Pugliese, K. Jordan, H. Cederberg, J. Brohult, J Altern Complement Med (1998), 4, 87-99.
- [3] R. Andreesen, Prog Biochem Pharmacol, (1988), 22, 118-31.
- [4] W. E. Berdel, Br J Cancer, (1991) 64, 208-211.
- [5] L. Diomedea, F Colotta, B Piovani, F Re, E. J. Modest, M. Salmona, Int J Cancer, (1993) 53, 124-130.
- [6] J. Palmblad, J. Samuelsson, J. Brohult, Scand J Clin Lab Invest, (1990) 50, 363-70.
- [7] K. Hartvigsen, A. Ravandi, R. Harkewicz, H. Kamido, K. Bukhave, G. Hølmer, A. Kuksis, Lipids (2006) 41, 679-693.
- [8] A. Tokumura, Prog Lipid Res (1995) 34, 151-184.
- [9] A. Toscani, D. R. Soprano, K. J. Soprano, Oncogene Res. (1988), 223-238.
- [10] L. A. Mickley, S. E. Bates, N. D. Richert, S. Currier, S. Tanaka, F. Foss, N. Rosen, A. T. Fojo, J Biol Chem (1989) 264, 18031-18040.
- [11] C. W. Taylor, Y. S. Kim, K. E. Childress-Fields, L. C. Yeoman, Cancer Lett (1992) 62, 95-105.
- [12] A. Wachtershauser, S. M. Loitsch, J. Stein, Biochem Biophys Res Commun (2000) 272, 380-385.
- [13] A. Hague, G. D. Diaz, D. J. Hicks, S. Krajewski, J. C. Reed, C. Paraskeva, Int J Cancer (1997), 72, 898-905.

- [14] Y. Tanaka, K. K. Bush, T. Eguchi, N. Ikekawa, T. Taguchi, Y. Kobayashi, P. J. Higgins, *Arch Biochem Biophys* (1990) 276, 415–423.
- [15] M. Yoshida, Y. Tanaka, T. Eguchi, N. I. kekawa, N. Saijo, *Anticancer Res* (1992) 12, 1947–1952.
- [16] J. Stein, O. Schröder, V. Milovic, W. F. Caspary, *Gastroenterology* (1995) 108, 673–679.
- [17] O. Schröder, J. Opritz, J. Stein, *Digestion* (2000) 62, 152–158.
- 18 J. Stein, M. Zores, O. Schröder, *Eur J Nutr* (2000) 39, 121–125.
- [19] C. Schröder, K. Eckert, H. R. Maurer, *Int J Oncol* (1998) 13, 1335–1340.
- [20] N. Satya Sree Kolar, R. Barhoumi, J. R. Lupton, R. S. Chapkin, *Cancer Res* (2007) 67, 5561–5568.
- [21] N. Yeevoon, R. Barhoumi, R. B. Tjalkens, Y. Fan, S. Kolar, N. Wang, J. R. Lupton, and R. S. Chapkin, *Carcinogenesis* (2005) 26, 1914–1921.
- [22] C. F. Torres, L. Vazquez, F. J. Señorans, G. Reglero. *Process Biochem* (2009) 44, 1025–1031.
- [23] R. M. Blanco, P. Terreros, N. Muñoz, E. Serra, *J Mol Catal B Enzym* (2007) 47, 13–20.
- [24] F. X. Malcata, C. G. Hill, Jr., C. H. Amundson, *Biotech Bioeng* (1992) 39, 984–1001.
- [25] L. P. Lessard, C. G. Hill, Jr. *Biotech Bioeng* (2000) 69, 183–195.
- [26] C. F. Torres, M. Moeljadi, C.G. Hill, Jr., *Biotechnol Bioeng* (2003) 83, 274–281.
- [27] Y. Yesiloglu. *J Am Oil Chem Soc.* (2004) 81, 157–160.
- [28] Y. Shimada, Y. Watanabe, A. Sugihara, Y. Tominaga, *J Mol Catal B Enzym* (2002) 17, 133–142.

[29] W. Piyatheerawong, Y. Iwasaki, T. Yamane, J Chromatogr A
(2005) 1068, 243-248.